Newborn reactions to maternal prenatal stress alter umbilical cord blood tRNA fragments targeting cholinergic transcripts

Shani Vaknine Treidel[1,4], Silvia M. Lobmaier[2], Ritika Sharma[2,3], Nimrod Madrer[1], Dana Shulman[1], Pnina Greenberg[1], Estelle R. Bennett[1], David S. Greenberg[1], Camilla Zelgert[2], Peter Zimmermann[2], Martin G. Frasch[5], Liran Carmel[4], Marta C. Antonelli[2,6], and Hermona Soreq[1*]

1. Department of Biological Chemistry and the Edmond and Lily Safra Center of Brain Science, the Hebrew University of Jerusalem, Jerusalem, Israel.
2. Department of Obstetrics and Gynecology, Technical University of Munich, Munich, Germany.
3. Helmholtz Centre Munich, German Research Center for Health and Environment (GmbH), Munich, Germany.
4. Department of Genetics, the Hebrew University of Jerusalem, Jerusalem, Israel.
5. Department of Obstetrics and Gynecology, University of Washington, Seattle, United States.
6. Instituto de Biología Celular y Neurociencias "Prof. E. De Robertis", Facultad De Medicina, UBA, Buenos Aires, Argentina.
*Corresponding author to whom correspondence should be addressed: Hermona Soreq, email, hermona.soreq@mail.huji.ac.il

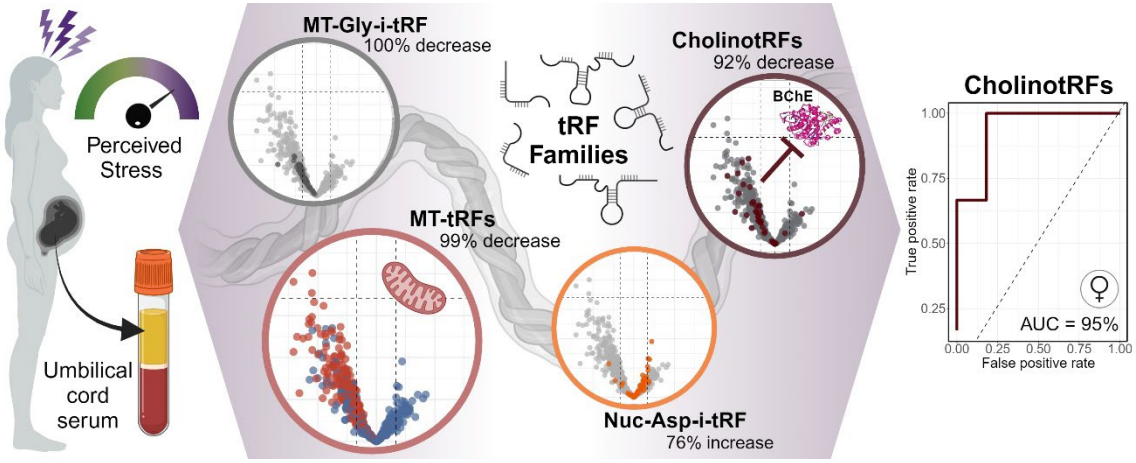

1 Abstract

Maternal perceived prenatal stress (PPS) is a known risk factor for diverse developmental impairments in newborns, but the underlying molecular processes are incompletely understood. Here, we report that PPS responses altered profiles of blood transfer RNA fragments (tRFs), 16-50nt long non-random cleavage products of tRNAs at birth. Moreover, maternal and umbilical cord serum from stressed and control mothers and their newborns presented selective enrichment of particular tRF families grouped by their mitochondrial or nuclear genome origin, coded amino acid and cleavage type. Suggesting a sex-specific effect, grouped tRF families revealed shared length and expression patterns which were strongest in the female newborns. Of those, some tRFs carried complementary motifs to specific cholinergic mRNAs, indicating possible translational regulation similarly to microRNAs. Compatible with the cholinergic regulation of stress reactions, those "CholinotRFs" achieved AUC of 95% when classifying female newborns according to maternal PPS. Correspondingly, we found altered catalytic activity of serum acetylcholinesterase, an effect which was elevated in male newborns, marking a second sex-specific impact. Our findings indicate association of tRF families' patterns with newborns sex-specific stress response to PPS, and may lead to better diagnosis and therapeutic tools for these and other stressors.

2 Introduction

The womb environment plays a crucial role in determining the future physical and mental health of the fetus. Many factors influencing this environment have been shown to affect fetal development (1–7). Specifically, psychosocial stress in the form of clinical or preclinical prenatal depression or anxiety has been shown to affect 20% of all pregnancies (8–10). As psychological stress is difficult to measure directly due to its subjective nature, it can be evaluated using perceived stress measurement (10, 11). Indeed, prenatal perceived stress (PPS) has been associated with offspring neurodevelopmental impairments, including escalated neurobehavioral problems and greater vulnerability towards developing psychiatric disorders later in life (12, 13). Moreover, PPS was negatively correlated with fetal left hippocampal volume (14, 15), infant cognitive performance at 18 months (8), and newborn telomeres length (16, 17). In some cases, these effects were shown to be sex-specific, pointing mainly at male newborns as more vulnerable (9, 18). Proposed mechanisms mediating these effects include epigenetic programing (19) and maternal immune activation through the hypothalamic-pituitary-adrenal axis (HPA), but cortisol-mediated fetal programming presented conflicting evidence (10, 20, 21). However, little is known about the role of short noncoding RNAs in these processes.

tRNA fragments (tRFs) are short noncoding RNAs cleaved from pre- and mature tRNAs by specific endonucleases. Their length ranges from 16 to 50 nucleotides and they are highly conserved across the evolutionary tree (22, 23). Human tRNA genes originate from both the nuclear and the mitochondrial (MT) genomes, and both are important for healthy cell function (24). Moreover, the nuclear genome contains "lookalike" tRNA genes, mimicking MT tRNAs, hailing their functional importance also outside of the mitochondria (25). The more widely studied tRFs are cleaved from mature tRNAs, and are classified into five groups based on their cleavage point: 5'-half and 3'-half tRFs are produced by angiogenin cleavage at the anticodon loop, splitting the tRNA into two halves, whereas 5'-tRFs, i-tRFs, and 3'-tRFs are cleaved around the D- and T-loops by a combination of angiogenin, dicer and other endonucleases, splitting the tRNA into three parts (24, 26). Interestingly, these cleavage points are not precise and can vary across tRFs sharing their cleavage type (24), sometime influenced by tRNA modifications, such as methylation and pseudouridylation, which are actively involved in the biogenesis of tRFs (23, 27). Further, tRFs can act as regulators of transcription and translation by various mechanisms, among them complementary binding to other RNAs or to RNA binding proteins, promotion of ribosome biogenesis, and post-transcriptional gene silencing via the

RISC complex (23, 26–28). The roles of tRFs have been explored in neurodegenerative diseases, cancers, stroke and non-alcoholic fatty liver disease (27, 29–32), but very few studies explored their impact on pregnancy complications or developmental disorders (33, 34).

The cholinergic system controls cognitive processes, inflammatory events, and neuromuscular communication (35–37). It is also a major regulator of stress responses and as such it plays a role in trauma reactions, neurodegenerative disease, stroke, and other mental conditions (38, 39). As a major player in both the central and the peripheral nervous system, acetylcholine is produced in neurons as well as in liver and immune cells and is hydrolyzed by cholinesterase enzymes. The major cholinesterase in the brain is acetylcholinesterase (AChE) and in the periphery, butyrylcholinesterase (BChE) (35, 36). Shifts in the balance between the activities of these two enzymes in the circulatory system have been shown to reflect different conditions, from anxiety to Alzheimer's disease (38). Notably, the expression of these and other cholinergic genes is regulated in several psychological disorders by "CholinomiRs" (40), microRNAs (miRs) targeting cholinergic genes (36, 41, 42). Interestingly, tRFs as well may participate in regulating the cholinergic genes via similar mechanisms. Circulating "CholinotRFs" are elevated while CholinomiR levels decline in nucleated blood cells from patients two days post-ischemic stroke (31), and mitochondrial-originated CholinotRFs show a sex-specific decline in the nucleus accumbens of women with Alzheimer's disease (29).

Based on these and other studies, we hypothesized that CholinotRFs may present a promising avenue to study newborns reactions to PPS. This study is a part of the 'FELICITy' study collection (43–46), exploring the influence of PPS on the fetus. This unique cohort explores roughly 120 mother-baby dyads using a comprehensive battery of biomarkers, with the goal of identifying the stressed newborns at as early a stage as possible. Previous studies yielded the fetal stress index (FSI), a measurement of the fetal heart rate reactivity in response to fluctuations in the maternal heart rate measured in the third trimester, maternal hair cortisol levels at birth (46), umbilical cord serum (UCS) iron homeostasis biomarkers (45), and DNA methylation in newborn saliva (44). All of these biomarkers presented differences between stress and control groups, some in a sex-specific manner, as in the case of transferrin saturation levels which were changed only in male newborns in the PPS group (45).

Here, we describe an in-depth exploration of the PPS impact on the newborn. We tested if and how modulated levels of tRFs and cholinesterase enzymes in mothers and offspring at birth reflect maternal stress levels as assessed by PPS during the third trimester. As the earliest indicators of newborns' reaction to PPS, we explored both serum cholinesterase activities and

short RNA-sequencing profiles of short noncoding RNAs in the mothers' serum and their newborns' UCS. Using this multi-leveled approach, we identified sex-specific differences in particular tRF families and in cholinesterase activities which differentiate between newborns of stressed and non-stressed mothers. Importantly, our analysis pipeline showed that grouping tRFs into families based on shared properties is more informative than considering each tRF type separately. Finally, we showed that CholinotRF enabled accurate classification of female newborns according to their PPS condition.

3 Materials and methods

3.1 Participant recruitment and sample collection

A cohort of 18 - 45 years old women with singleton pregnancies was recruited (July 2016 - May 2018) by the Department of Obstetrics and Gynecology at Klinikum Rechts der Isar Hospital of the Technical University of Munich, as part of the FELICITy project (45, 46). PPS was assessed during their early third trimester using the Cohen Perceived Stress Scale (PSS-10) questionnaire (11). Based on a pilot study, women who achieved PSS < 19 were assigned to the control group and those with PSS ≥ 19 to the PPS group (46). The women also completed the prenatal distress questionnaire (PDQ) (47) that assesses pregnancy-related stress and was highly correlated with PSS-10 scores (Supplementary Figure 1c). 728 women filled the PSS-10, and at the day of the birth venous maternal blood was collected from 128 of them upon entry into the delivery room and umbilical cord blood (arterial or venous) was collected from 120 newborns post-partum. All blood samples were collected into 9 mL S-Monovette® Serum Gel with Clotting Activator tubes (Sarstedt, # 02.1388). Serum was separated by a 10 minutes centrifugation at 2500 RPM, then frozen at -20°C and kept for a long term at -80°C. Samples were shipped on dry ice to the Soreq lab at the Hebrew University of Jerusalem, where they were kept at -80°C until analysis.

3.2 RNA extraction

Serum samples from both maternal and newborn bloods served for extracting short RNA. Samples were defrosted at room temperature, a 500µL aliquot was removed and centrifuged at 4°C, 3000g, for five minutes, and RNA was extracted from 200uL taken from the top of the aliquot, using the miRNeasy Serum/Plasma Advanced Kit (Qiagen, 217204) according to the manufacturer's instructions. Concentration was determined (NanoDrop 2000, Thermo Scientific) with an average yield of 14.3 ng/µL. Quality was assessed (Bioanalyzer 6000,

Agilent) with average RIN values of 1.8. Importantly, these low values are due to the almost complete lack of rRNA in serum (48) and do not reflect poor quality.

3.3 Sequencing and alignment

Of the 120 UCS samples, only those of dyads with the mother scoring either low (PSS-10 ≤ 10) or high (PSS-10 ≥ 19) PPS were considered for short RNA sequencing (Supplementary Figure 1a). The samples were divided into four groups by the mothers' PSS-10 score and the newborn sex, and for each group the 12 samples with the highest RNA concentration in both NanoDrop and Bioanalyzer assessment were chosen for subsequent sequencing (n=48). Post-sequencing, four samples were disqualified due to extremely low or high counts. Further, only UCS RNA samples from vaginal non-emergency births (58.3%, Supplementary Figure 1b) were analyzed, to prevent birth types from confounding the sequencing results. This created a subset of 35 newborn RNA samples, divided into four groups: female and male newborns from PPS mothers (female stress, n = 6; male stress, n = 8) and female and male newborns from control mothers (female control, n = 11; male control, n = 10). A subset of 24 samples from mothers corresponding to the sequenced newborns was chosen to form matched dyads (n = 6 in all four groups), based on the highest RNA concentration in the maternal cohort.

Libraries were constructed using the D-Plex Small RNA-seq Kit from Illumina (Diagenode, C05030001) and the short RNA fraction was sequenced on the NextSeq 500 System (Illumina) at the Center for Genomic Technologies Facility, the Hebrew University of Jerusalem. Newborn and maternal samples were sequenced on separate flow cells (NextSeq 500/550 High Output Kit v2.5 75 Cycles, Illumina, 20024906) using 1600 pg/sample in the newborn cohort and, due to lower RNA yield, 400 pg/sample in the maternal one. To compensate for the difference, sequencing depth was ~10M reads for newborns and ~20M for maternal samples. Subsequent quality control was re-assessed using FastQC (49) version 0.11.8, with Cutadapt (50) for removing the adaptor sequences, followed by Flexbar (51, 52) for further quality screening and cleaning. Subsequent tRF alignment was done using MINTmap (53) to MINTbase v2.0 (54) and microRNA alignment was done using miRDeep2 (55) to miRbase 22.1 (56–61).

3.4 Assignment of tRF families

tRFs share sequence similarities due to their shared tRNA origin and production mechanism (24). In our study, we used these characteristics as grouping factors, assigning different tRFs that share genome origin (mitochondrial or nuclear), coded amino acid (as referenced by the parental tRNA gene), and cleavage type (5'-tRF, 5-half, i-tRF, 3-half, 3'-tRF) (54), to the same “tRF family". Using the multiple sequence alignment (MSA) algorithm in the msa R package

(62) we sought sequence similarities of all tRF families represented in our newborns data which had more than one member (45 out of 51 families). Of those families, 43 enabled us to produce a consensus sequence that coincided with a real tRF, and our data included 42 of these "consensus tRFs" that were 16-27nt long (Supplementary table 1, Supplementary Figure 2). It is important to note that we did not find a sequence motif that was shared between all tRF families. Furthermore, unlike the nuclear genome that contains multiple tRNA genes for each amino acid, the mitochondrial (MT) genome carries only one tRNA gene for each amino acid, apart from leucine and serine with two each, and each tRNA can encode groups of four closely related codons due to an unmodified uridine at the wobble position among other related mechanisms (25, 63). As the majority of our data was comprised of those MT tRFs which are coded in the MT-DNA mostly by a single codon, it sufficed to classify tRFs according to the parental tRNA coded amino acid (Supplementary Figure 3a). Even so, we could show that multiple tRF families constructed from nuclear tRNA genes representing different codons showed similar sequences and united expression patterns (Supplementary Figure 2, Figure 3). In addition, length distribution analysis was performed as follows: mean expression levels of each tRF family under each length it spans was calculated for each participant. Next, Kruskal Wallis test was used for each of the tRF families separately, followed by FDR correction, to compare their mean expression between the stress-by-sex groups. Together, these steps enabled us to assess the differences between specific tRF families rather than individual tRFs.

3.5 Cholinesterase activity measurements

Cholinesterase activity was measured in serum samples from 70 mothers and newborns who experienced normal vaginal birth using Ellman's assay (64). Briefly, each sample was defrosted rapidly in a water bath, diluted 1:20 in phosphate buffered saline (PBS), and 10 µL were mixed with 180 µL Ellman's solution in 96 flat-well plates. Tests were all performed in triplicates. Each plate was incubated either without inhibitors, or with the BChE inhibitor tetraisopropylpyrophosphoramide (iso-OMPA; final concentration 50 µM; Sigma, T1505), or the AChE inhibitor BW284c51 (final concentration 5 µM; Sigma, A9103). To enable comparison between plates, each plate included four internal controls: (1) a random maternal sample, (2) its corresponding newborn sample, (3) a recombinant AChE protein sample, and (4) a recombinant BChE protein sample. The first two served as normalizing controls and the last two as internal controls. The iso-OMPA plates alone were incubated for 120 minutes covered in aluminum foil, and in all plates 10 µL acetylthiocholine were added to all wells immediately before measurement. Absorbance at 436 nm was read in a microplate reader (Tecan Spark,

Tecan Group, Switzerland) at room temperature for 21 kinetic cycles of one minute each. The kinetic measurements were retrieved using the SparkControl Magellan 3.1 program and were further analyzed using R (65). Average values of samples in "mean OD/minute" units were converted to units of “nmol substrate hydrolyzed per minute per ml” using the Beer-Lambert law (A= εlc; molar absorptivity constant ε 2-nitro-5-thiobenzoate= 13,600), multiplied by the serum dilution factor (1:20). Normalization between plates was based on the maternal and newborn control samples described above and was performed separately for maternal and newborn samples. Values were log-transformed to minimize the effect of outliers on the mean. The normalization factor of plate i, denoted f_i, is computed by

$$f_i = \frac{\sum_{j=1}^{n} \log\left(control_j\right)}{n} - \log(control_i),$$

where n is the number of plates. Let $s_{i,k}$ be the activity of the non-control sample k in plate i. The normalized activity, denoted $s'_{i,k}$, is computed by

$$s'_{i,k} = s_{i,k} \cdot e^{f_i}.$$

3.6 Statistical analysis

3.6.1 Differential expression analysis

Differential expression (DE) analysis was performed using DESeq2 (66) package in R with their suggested prefiltering step, disqualifying all miRs and tRFs that did not achieve rowSums(counts(dds) >= 10) >= smallestGroupSize, where smallestGroupSize=6. DESeq2 normalization was used and findings were deemed statistically significant for $p \leq 0.05$ after FDR correction using Wald’s test. This filter left 565 and 174 tRFs and 69 and 49 miRs for downstream analyses in newborn and maternal samples, respectively.

3.6.2 Identification of cholinergic targets

To identify miRs and tRFs that target genes in the cholinergic network we used the miRDB sequence-based prediction algorithm (67, 68) combined with a modified version of our in-house cholinergic scoring system (29–31). Briefly, all miRs and tRFs that were 17-28 nucleotides long were tested and miR/tRF targets with a prediction score ≥ 80 were matched against a list of 102 cholinergic genes (Supplementary table 2) which were assigned scores of one or five according to their role in the cholinergic network, with core genes (e.g. CHAT, ACHE) receiving a score of five and others (e.g. IL6, CHKB) receiving a score of one. For each miR/tRF a "cholinergic score" was calculated by summing the scores of their target genes, and

all miRs/tRFs with a score of five or higher were denoted as CholinomiRs/CholinotRFs. This cutoff was chosen to identify as cholinergic (a) miRs or tRFs which target core cholinergic genes and (b) miRs or tRFs which target at least five peripheral cholinergic genes.

3.6.3 Classification and visualization

SVM kernel classification was employed using the Caret R package (69) with a "leave-one-out" cross validation method, and the MLeval R package (70) was used to calculate receiver operating characteristic (ROC) curve, area under the curve (AUC), accuracy, precision, and F1 and recall values (Supplementary table 8). P-values and subsequent false discovery rate (FDR) were calculated based on 10,000 permutations for five of the top marker groups (Supplementary table 9).

4 Results

4.1 tRNA fragment families distinguish between newborn stress and control groups, with a stronger effect in females

To study the influence of PPS on the newborn reaction to the birth stress, we studied serum samples collected from mothers and umbilical cord blood within the FELICITy cohort (43–46). The women participants went through two forms of psychological stress assessments during the third trimester, first assessing their perceived stress by the Cohen perceived stress scale (PSS-10) (11), and second assessing their pregnancy-related stress using the prenatal distress questionnaire (PDQ) (47). The stress groups were assigned according to the PSS-10 values, and the two questionnaire scores were predictably highly correlated (Supplementary Figure 1c). Other than those two questionnaires, no demographic or medical feature of the cohort differed significantly between these tested groups (Figure 1b, Supplementary Figure 1d).

Comparing the tRF profiles between newborn stress and control groups (males and females together), divided according to the mother's PPS as measured by the PSS-10 questionnaire, revealed three differentially expressed (DE) tRFs (Figure 2b). Repeating the analysis while accounting for the newborn sex found four DE tRFs separating female newborns, all of which intriguingly differed from the three tRFs identified in the previous comparison (Figure 2d). Notably, the expression of all seven DE tRFs decreased in the stressed group. No DE tRFs were identified when comparing male newborns alone (Figure 2h).

a.

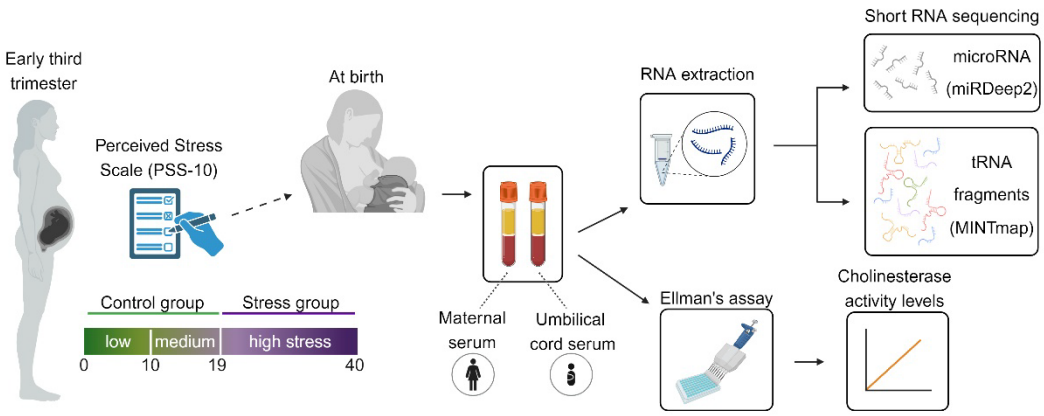

b.

Maternal psychological stress	Control (ctl)		Stress	
Newborns' sex	Female (N=19)	Male (N=23)	Female (N=14)	Male (N=14)
PSS score				
Mean (SD)	8.37 (4.07)	9.13 (3.79)	23.2 (3.12)	23.1 (3.61)
Median [Min, Max]	9.00 [1.00, 18.0]	10.0 [0, 15.0]	23.5 [19.0, 31.0]	22.0 [19.0, 32.0]
PDQ score				
Mean (SD)	8.89 (5.12)	7.26 (4.71)	15.8 (8.03)	15.6 (6.79)
Median [Min, Max]	9.00 [2.00, 20.0]	6.00 [3.00, 25.0]	16.5 [4.00, 35.0]	13.5 [8.00, 28.0]
Maternal age at study entry				
Mean (SD)	33.5 (3.47)	33.3 (3.25)	30.4 (5.02)	32.6 (4.16)
Median [Min, Max]	34.0 [28.0, 41.0]	33.0 [28.0, 39.0]	31.0 [21.0, 39.0]	31.5 [27.0, 38.0]
Maternal BMI at third trimester				
Mean (SD)	26.7 (2.58)	26.5 (3.45)	27.8 (4.42)	30.6 (5.60)
Median [Min, Max]	25.8 [23.0, 31.3]	26.2 [20.5, 37.3]	26.9 [21.2, 38.1]	28.8 [25.3, 43.2]
Maternal BMI before pregnancy				
Mean (SD)	21.9 (2.50)	22.0 (3.44)	23.1 (3.91)	25.5 (5.54)
Median [Min, Max]	21.0 [18.6, 27.4]	21.5 [18.2, 35.0]	22.4 [16.8, 31.9]	24.2 [20.0, 38.3]
Gestational age at birth (week)				
Mean (SD)	40.1 (1.12)	39.6 (1.05)	39.5 (0.909)	40.0 (1.01)
Median [Min, Max]	40.4 [37.7, 41.4]	39.6 [37.7, 41.7]	39.6 [37.7, 40.7]	40.1 [37.9, 41.4]
Number of births				
Mean (SD)	0.842 (0.765)	0.739 (0.752)	0.500 (0.519)	1.14 (1.29)
Median [Min, Max]	1.00 [0, 2.00]	1.00 [0, 2.00]	0.500 [0, 1.00]	1.00 [0, 4.00]
Apgar 5				
Mean (SD)	9.89 (0.315)	9.65 (0.714)	9.79 (0.579)	9.36 (0.745)
Median [Min, Max]	10.0 [9.00, 10.0]	10.0 [7.00, 10.0]	10.0 [8.00, 10.0]	9.50 [8.00, 10.0]
Newborn head circumference (cm)				
Mean (SD)	34.7 (0.632)	35.1 (1.46)	34.6 (1.29)	35.8 (1.46)
Median [Min, Max]	35.0 [34.0, 36.0]	35.5 [32.0, 38.0]	35.0 [32.0, 36.5]	35.5 [33.0, 38.0]
Newborn weight (gram)				
Mean (SD)	3520 (322)	3530 (376)	3430 (377)	3760 (438)
Median [Min, Max]	3530 [2880, 4150]	3540 [2960, 4490]	3410 [2680, 3950]	3820 [3020, 4490]

Figure 1 – Study layout and participant characteristics. (a) Mothers recruited early in the third trimester were assigned to psychosocial stress and control groups based on the Cohen Perceived Stress Scale 10 (PSS-10). Maternal blood (n=128) samples were collected upon entry into the delivery room and umbilical cord blood samples (n=120) were collected postpartum. Serum was extracted and served for ChE activity measurements and short RNA sequencing. Only mother-newborn dayds who had normal vaginal deliveries were used for subsequent analyses (Supplamentary figure 1). (b) The four groups reflect combinations of maternal PPS scores and newborn sex. Maternal and newborn parameters pertinent to the study are presented with both mean and median. Created with BioRender.

Due to their shared genomic origin, parental tRNA coded amino acid, and cleavage type, diverse tRFs often present sequence similarity (Figure 2a) (24), unlike microRNAs (miRs), and may hence share similar functions. Further, diverse tRFs are simultaneously produced from

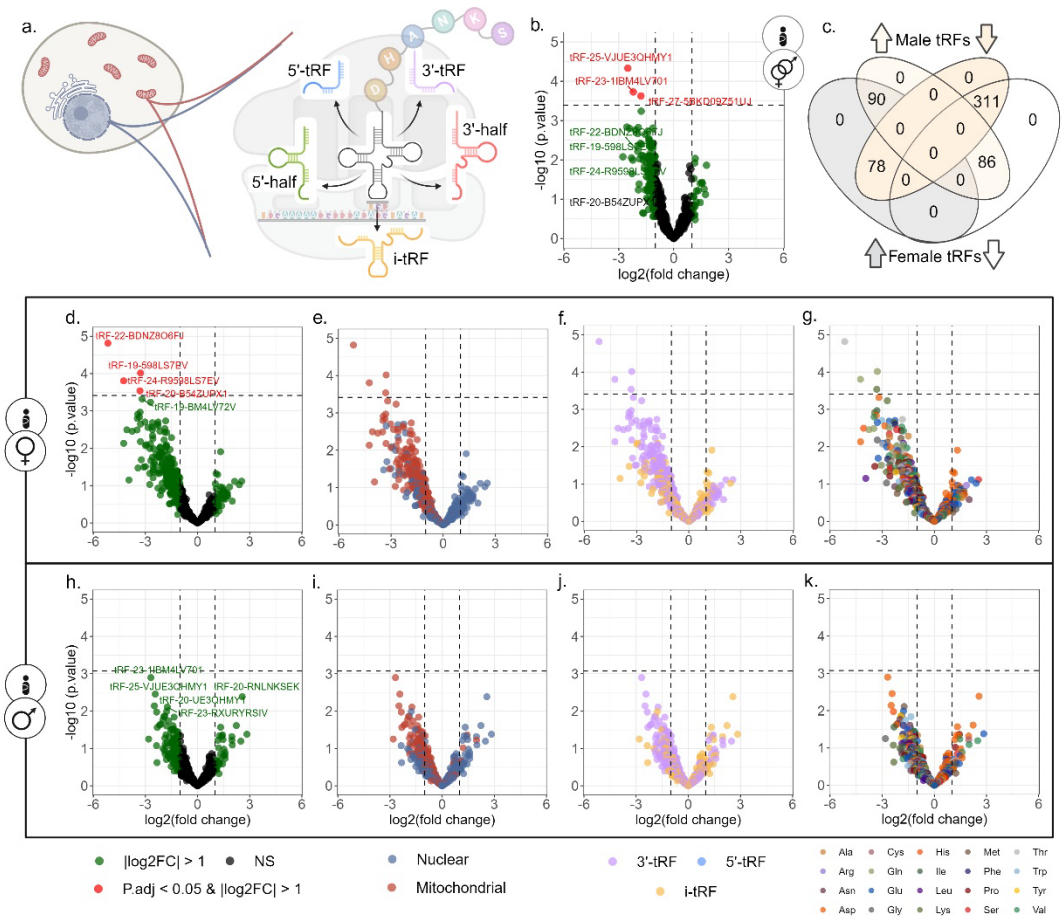

Figure 2 - tRF patterns differentiate stressed and control newborns, with a stronger effect seen in females. (a) tRNA genes are transcribed from two genome origins, nuclear (Nuc) and mitochondrial (MT), and encode specific amino acids. The mature tRNA is cleaved in specific locations, producing the five subtypes of tRFs: 5'-tRF, 5-half, i-tRF, 3'-half, and 3'-tRF. (b, d, h) Volcano plots of DE tRFs in stressed vs. control male and female newborns together (n=14 vs. 21), in stress vs. control females (n=6 vs. 11), and in stress vs. control males (n=8 vs. 10). (c) Venn diagram of overlapping tRFs with increasing and decreasing levels in the male and female comparisons. (e, i) Volcano plots with tRFs colored according to genomic origin, (f,j) cleavage type, (g,k) and tRNA coded amino acid. Created with BioRender.

tRNAs by distinct nucleases (1–7). Therefore, we hypothesized that bulks of similar tRFs may be produced and function together, creating "tRF storms" (31). Should that be the case, traditional DE analysis, which regards each tRF as an independent transcript, might fail to identify trends that would characterize whole “tRF families” whose joint biological impact may be considerable. To this end, we added family information to the tRFs analysis, which enabled the identification of tRF families that separate stressed and control female and male newborns (Figure 2e-g). Using this approach, we revealed a profound decline in the levels of mitochondrial (MT) genome-originated tRFs in stressed female newborns, with 98.9% of the tRFs showing negative fold-change (Figure 2e,i; exact binomial test FDR = 8.21E-74). A similar, albeit less pronounced trend, was observed in male newborns, where 90% of MT tRFs showed negative fold-change (Figure 2i; FDR = 9.06E-44). Declined levels were also apparent in both sexes in 3'-tRFs (Figure 2f,j; 73.6% in females, FDR = 3.38E-18; 74.5% in males, FDR = 1.73E-

19), and in i-tRFs (65.5% in females, FDR = 7.66E-06; 59.6% in males, FDR = 0.0064). Additionally, tRF families grouped by their coded amino acids showed varying trends as well (Figure 2g, k; Supplementary table 3).

Interestingly, repeating the analysis in the maternal cohort revealed no DE tRFs in any of those comparisons (Supplementary Figure 4a, e, i). Yet, tRF family patterns differed from those of the newborns, revealing a decline in nuclear genome-originated (Nuc) tRFs (Supplementary Figure 3j; 71.1%, exact binomial test FDR = 2.1E-03) and i-tRFs (Supplementary Figure 4k; 80.9%, FDR = 4.5E-04) in stressed mothers, especially of male newborns (Supplementary Figure 4b-c; Nuc: 64.5%, FDR = 4.6E-02; i-tRFs: 76.6%, FDR = 2.1E-03). Moreover, the maternal cohort showed globally altered levels of tRF-halves, which did not emerge in newborns (Supplementary Figure 4c, g, k). In particular, 3'-halves showed significantly elevated levels both in stressed mothers in general (87%, FDR = 2.2E-03) and in stressed mothers of male newborns specifically (78.3%, FDR = 3.8E-02). Importantly, only 19 out of 45 tRF families in newborns and 30 in mothers were found in both cohorts. Moreover, the tRNA genes from which those tRFs were derived (according to the alignment by MINTmap) did not fully match the most prevalent tRNA genes, as shown by GtRNAdb (71, 72) for Nuc tRNA genes and by mitotRNAdb (73) for MT tRNA genes (Supplementary Figure 3a). Furthermore, tRF families with significantly modified trends did not necessarily coincide with the expected tRF families by MINTmap (Supplementary Figure 3b). This phenomenon has been seen previously (27), although to the best of our knowledge was not studied directly, and adds to the notion that tRFs production is not random but rather occurs in families.

4.2 tRF families in newborns and maternal serum present specific expression patterns

To test the working hypothesis that specific tRF families function as groups based on their genome origin, parental tRNA coded amino acid and cleavage type, we tested whether those tRF families show shared stress-related changes in their expression levels. Indeed, exact binomial test (FDR ≤ 0.05) identified 24 tRF families with significant DE values (Supplementary table 3). The strongest signal observed showed declining levels of MT-originated Gly-i-tRFs (100% in stressed female newborns, FDR = 3.5E-16; 96.6% in stressed male newborns, FDR = 6.1E-13). Elevated levels of the nuclear genome-originated Asp-i-tRFs were strong as well (76.6% in stressed female newborns, FDR = 0.0025; 76.6% in male newborns, FDR = 0.009). In mothers, tRF families failed to present significant change (Supplementary table 4). However, comparing all stressed mothers to control mothers and mothers of male newborns alone

revealed a trend of declined expression of Nuc-Asp-i-tRFs (92.9%, FDR = 0.055 in both comparisons). Comparing the tRF families' effects between mothers and newborns revealed some cases of opposite trends of change (Figure 3b, Supplementary Figure5), emphasizing again the non-random patterns of tRF families and directing us towards seeking possible stress-related interaction between mothers and their newborns.

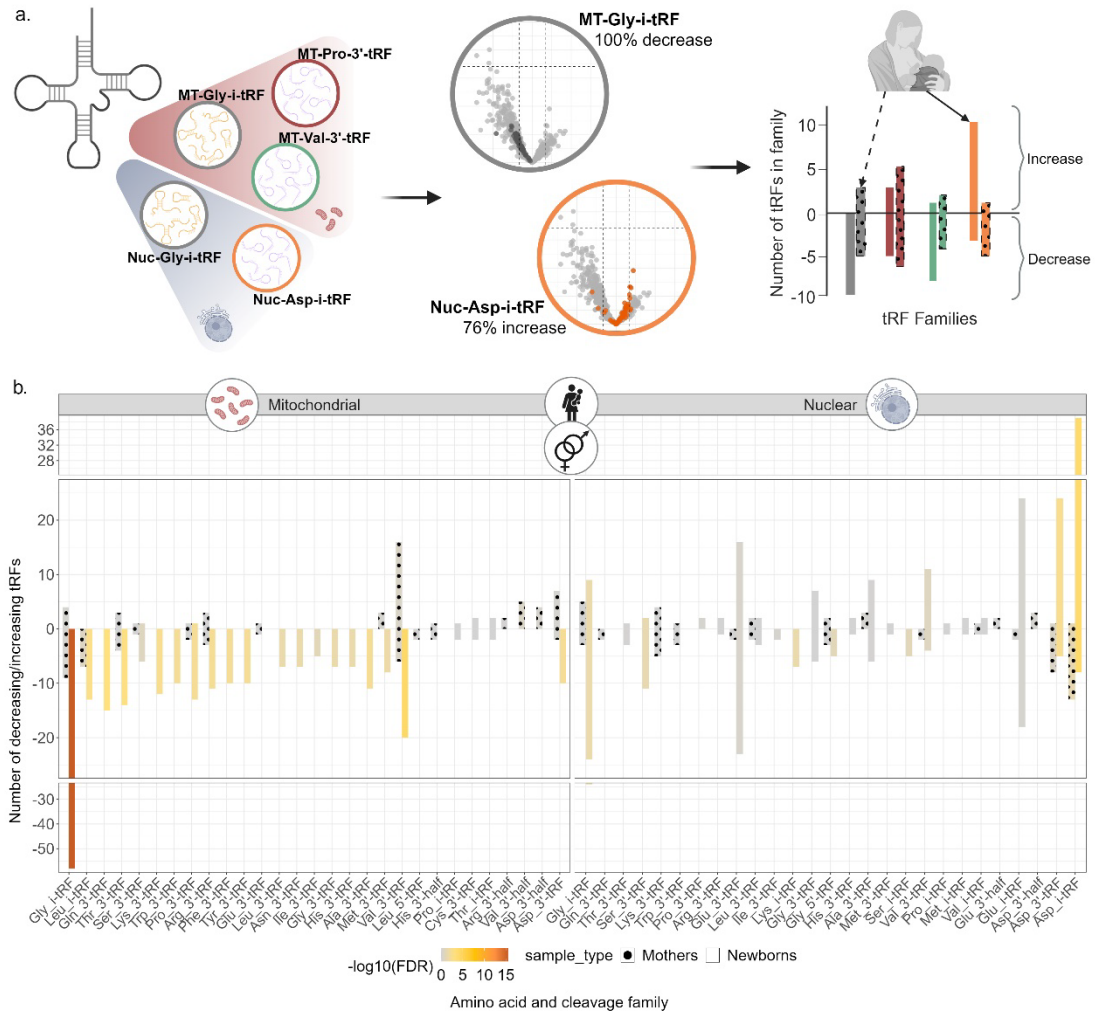

Figure 3 – tRFs families differ significantly between stressed and control groups, with some inverse effects between mothers and newborns. (a) tRF families were defined based on their genome origin, cleavage type, and parental tRNA coded amino acid. Only Ffamilies with one or more members were included in the analysis. The Exact binomial test (FDR ≤ 0.05) was used to quantify the tendency for decreased expression levels in the stress groups. (b) Bar plot presenting direction of change in each tRF family. Bar size reflects the number of tRFs in the identified family, with positive values indicating elevated levels and negative values indicating decreased levels in the stressed groups. Bar color indicates the significance level, empty bars depict newborns and patterned bars depict mothers. Created with BioRender.

Searching whether the expression of certain tRF families correlated to participant characteristics such as gestation age, newborn weight etc., revealed a strong correlation between the MT-Gly-i-tRF family and maternal BMI. 40 of the 59 members in this family showed high positive correlation between the tRF expression levels and maternal BMI during the third trimester, and 35 also correlated with the mothers' body weight at the same time

point (Supplementary table 5). Interestingly, the interaction between Glycine (Gly) and weight has been shown previously, with circulating Gly showing an inverse correlation with metabolic disorders such as obesity, non-alcoholic fatty liver disease, and type 2 diabetes (74–76). Moreover, Gly was shown to be important in late stages of pregnancy (77), and one of its related tRFs, the nuclear 5'-tRF-GlyGCC, was proposed as a regulator of obesity-associated pathways in human breast cancer cell lines, as well as mice and pigs (78, 79), altogether suggesting that these findings were not coincidental.

4.3 tRF families show distinct length distributions in stress groups

Dicer and Angiogenin, as well as other nucleases, cleave mature tRNAs to yield the five tRF subtypes (i-tRF, 3'-tRF, etc.), producing tRFs of various lengths under each cleavage category (24). To explore tRFs length distribution in our datasets, we first calculated the mean expression levels of all same-length tRFs in each newborn cohort (Figure 4a-b). Both male and female control groups presented non-even distribution of expression patterns, with a peak around the lengths of 23-24nt, and smaller peaks around lengths of 18-19nt and 31-32nt. The highest peak in all groups emerged at the length of 36nt, but was somewhat attenuated in the female stress group, which in general showed more even distribution of tRFs lengths. Intriguingly, the highest peak in the control groups overlapped known miR lengths, 16-28nt according to miRbase, (60) (Supplementary Figure 6a). Repeating the analysis for the mothers, we noticed far smaller differences in length distributions between stress and sex groups (Supplementary Figure 6b), suggesting that in newborns, more than in their mothers, tRFs tend to overlap miR lengths, possibly pointing at a shared functional role similar to that of miRs, by targeting mRNAs carrying a complementary sequence. Combined with the previous results, these findings indicate that mothers' perceived stress may lead to excessive reaction of her newborn that is reflected in declined tRFs levels.

Next, we tested whether newborn tRFs belonging to a particular family tend to appear in specific lengths, and if so, are those influenced by the mothers' PPS. For this purpose, we used the Kruskal-Wallis test on each tRFs family across the four stress-by-sex groups (Figure 4c). In newborns, we found numerous tRF families with significant preference both towards a single direction of expression change and a tendency for specific length distributions, whereas the maternal cohort showed no significant differences in length distribution between the groups. Notable was the MT-Gln-3'-tRF family, which showed elevation of tRF lengths in both control groups compared to the stress groups in newborns (Figure 4d), and in particular in females (Figure 4e). These results, together with previous evidence showing that tRFs production

reveals stress specificity (24, 26, 31), imply that tRNA cleavage into tRFs is context-specific, presenting differences between stress and sex groups already at birth.

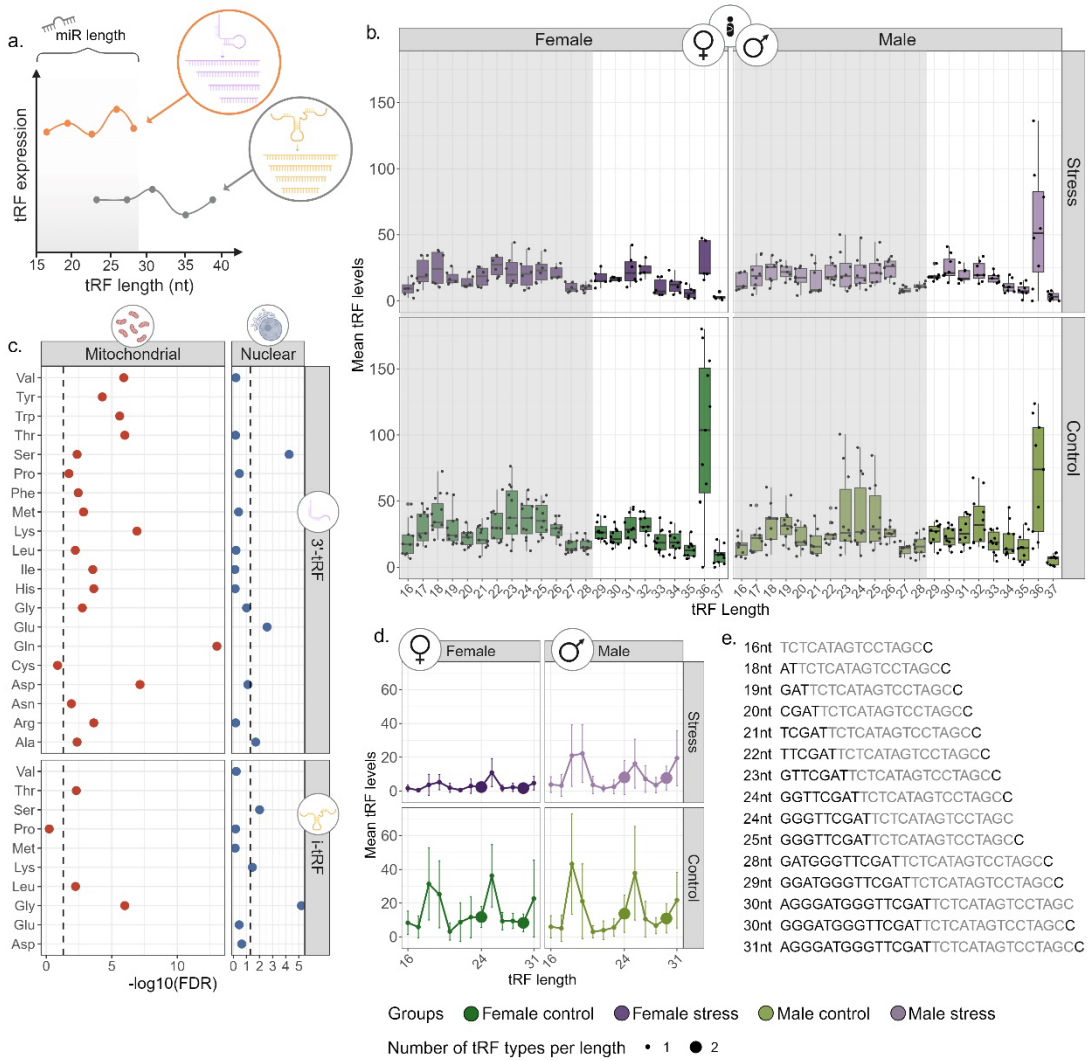

Figure 4 – tRF families differ in length across newborn stress and sex groups. (a) Illustration of tRF lengths and their overlap with miR lengths. (b) Boxplot showing mean expression levels of all tRFs of each length, calculated separately for the four stress-by-sex groups, with outliers identified and excluded from the analysis by the IQR method. The black dots represent mean values for single participants. The grey areas are lengths that overlap with miR length according to miRBase (16-28nt). (c) Kruskal-Wallis (KW) test of length distributions between the four groups, for each tRF family, of nuclear and mitochondrial origin. The dashed line marks the threshold of significance (FDR = 0.05). (d) Dot plot of the KW test for length distribution of the top tRF family, MT-Gln-3'-tRF, in each of the four groups. The length of tRFs in the family is plotted vs. their mean levels and the dot size reflects the number of tRFs sharing the same length in that family. (e) The sequences of all MT-Gln-3'-tRF family members in our data, from the shortest to the longest. Grey letters mark the sequence shared by all members. Created with BioRender.

4.4 microRNAs (miRs) present relatively small changes in the serum of newborns and mothers

To further explore our unique dataset, we carried out a similar analysis for serum miRs in the stress-by-sex groups, performed for both mothers and newborns (Supplementary Figure 7). Male newborns of PPS mothers showed elevated hsa-miR-7704 levels (Supplementary Figure 7a), which is also elevated in schizophrenia patients and may predict altered synapse activities

(80). Interestingly, one hypo-methylated CpG cg05306225 found in newborns saliva in a previous work of this cohort (44) was annotated to the CSMD1 gene, which was also found to be connected to schizophrenia (81–83). Furthermore, male and female newborns together revealed a stress-related decline in hsa-miR-301a-3p (Supplementary Figure 7b) predicted to control autoimmune cell differentiation through regulating STAT3 in multiple sclerosis patients (84). Decreased levels of hsa-miR-301a-3p emerged in males and females separately as well, but did not reach statistical significance. Two additional miRs, the hematopoietic regulating hsa-miR-223-3p (85, 86) and hsa-miR-142-5p (87, 88) showed declined levels in PPS mothers of female newborns (Supplementary Figure 7f). Moreover, 30 of the detected miRs were expressed in both mothers and newborns samples, hsa-miR-223-3p and hsa-miR-142-5p among them; hsa-miR-7704 and hsa-miR-301a-3p however, were unique to the newborns' samples.

All four DE miRs were previously connected to the immune system and to regulating cell division in various cancers (89–96). Interestingly, the two found in both umbilical cord and maternal serum were connected to pregnancies; hsa-miR-223-3p is highly expressed in plasma exosomes of 30 and 38 weeks normotensive pregnant women and was suggested to be one of the controllers of the fetal–maternal immune balance (97). In addition, hsa-miR-142-5p levels were increased in the serum of mothers whose fetuses suffered from fetal congenital diaphragmatic hernia at week 26 compared to controls. Further, hsa-miR-142-5p showed a general decline between 38-40 week and 24 hours after birth, and was suggested to be a fetal miR that has crossed to the maternal circulation (98). These results point again to the sex-specific effect reflected by short noncoding RNAs, evident even in the mothers of newborns of the opposite sex.

4.5 Stressed newborns show higher serum AChE levels

To explore the hypothesis that cholinergic signals in stressed mothers influence the newborns' reaction to birth stress, we have further tested the acetylcholine hydrolyzing cholinesterase (ChE) activities in the serum of both mothers and newborns. Interestingly, ChE activities did not differ between stressed and control mothers, possibly due to the timing in which the samples were drawn – at the beginning of the delivery, not afterwards like the UCS. However, stressed male and female newborns both showed higher serum acetylcholinesterase (AChE) activities than controls (Mann–Whitney U test: Female P-value = 0.035, male P-value = 0.0048), with males showing generally higher AChE activity compared to females (Figure 5d). Although not statistically significant, butyrylcholinesterase (BChE) activity in newborns

showed the same trend (Figure 5d). Together, these results suggest that serum acetylcholine levels in stressed newborns were predictably compromised compared to non-stressed ones.

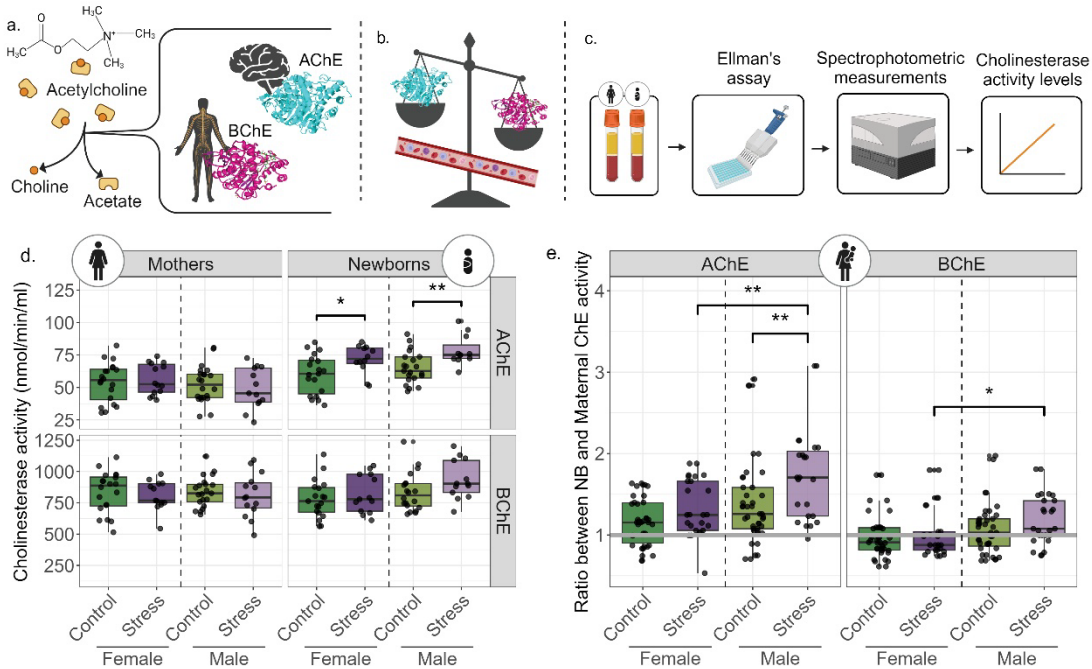

Figure 5 – Stressed newborns present altered ChE activities, reflecting cholinergic system involvement. (a) The cholinesterases AChE and BChE hydrolyze acetylcholine into acetate and choline. AChE is found predominantly in the brain and BChE in the periphery. (b) Balance between the two ChEs in the blood reflects different diseases and disorders. (c) Pipeline used to assess ChEs activities in our cohort. (d) Boxplots comparing AChE and BChE activities in the serum of mothers and newborns (AChE: mothers, n=69; newborns, n=63. BChE: mothers, n=68; newborns, n=67). (e) Ratios between newborn and mother couples for AChE (n=62) and BChE (n=64). The grey line indicates a ratio of one (equal ChE activities in mothers and newborns). P-values < 0.05, Mann–Whitney U test. IQR method to remove outliers was used in both d and e. Created with BioRender.

In all groups but female controls, we have further found higher AChE levels in newborns compared to their mothers (Wilcoxon signed rank test, FDR ≤ 0.05, Figure 5e, Supplementary table 6). Parallel findings emerged for females and males grouped separately, combining stress and control values (female FDR = 2.9E-03, male FDR = 2.8E-04). Furthermore, AChE activity was higher in stressed compared to control males (Mann–Whitney U test, P-value = 0.0072) and in stressed females compared to stressed males (P-value = 0.0087). For BChE activities, the newborn/mother ratio presented a similar trend between stressed males and females, with the male stress group showing higher levels (P-value = 0.041). Together, our findings identified higher AChE activity as an indicator of stronger response of the cholinergic system to birth stress in male newborns whose mothers suffered prenatal perceived stress compared to other newborns.

4.6 CholinotRFs and CholinomiRs show specific cholinergic predicted targets

Since tRFs may target genes similarly to miRs, and given the cholinergic stress-response network (35, 36), we sought the cholinergic gene targets of the identified tRFs and miRs. For this purpose, we used our previously established scoring system for cholinergic targets (Figure 6a) (29–31). Combined with the miRDB target prediction algorithm (22, 23), we identified 13 maternal and 16 newborns "CholinomiRs", showing enriched numbers compared to those expected based on the known miRs listed in miRbase 22.1v (Fisher's exact test, maternal and newborn P-values of 0.007 and 0.015, respectively). Similarly, we identified 13 maternal and 38 newborns "CholinotRFs", which were enriched in MT vs. Nuc tRFs in newborns (Fisher's exact test, P-value ≤ 0.00001). Intriguingly, these values support previous predictions in Parkinson's and Alzheimer's disease (29, 30), suggesting a wider connection between MT-originated tRFs and the cholinergic system in the context of both stress and neurodegeneration.

Next, we looked for potential overlaps between the predicted cholinergic gene targets of CholinomiRs (Supplementary table 8) and CholinotRFs (Supplementary table 7) in newborns (Figure 6b, c). Intriguingly, cholinergic genes belonging to the circadian sub-group and most cholinergic receptor genes were predicted to be targeted by both CholinomiRs and CholinotRFs. In contrast, key cholinergic genes encoding enzymes such as BChE and cytokines like IL6 were predicted to be targeted by CholinotRFs alone. However, Spearman correlations between BChE levels in newborns and mothers and its targeting tRFs did not reveal any significant correlations. Furthermore, specific tRF families showed larger inclination to target cholinergic genes, including 14 MT tRF families and three nuclear ones. Out of the 17 tRF families, only seven MT families had more than one member marked as CholinotRF. Specifically, MT-Thr-3'-tRF family members targeted genes across the entire cholinergic system, whereas the MT-Phe-3'-tRF family showed specificity toward only three of the cholinergic gene sub-groups. Moreover, the 14 newborn MT CholinotRF families presented specific length distributions, strengthening the notion of specific stress-driven tRFs production.

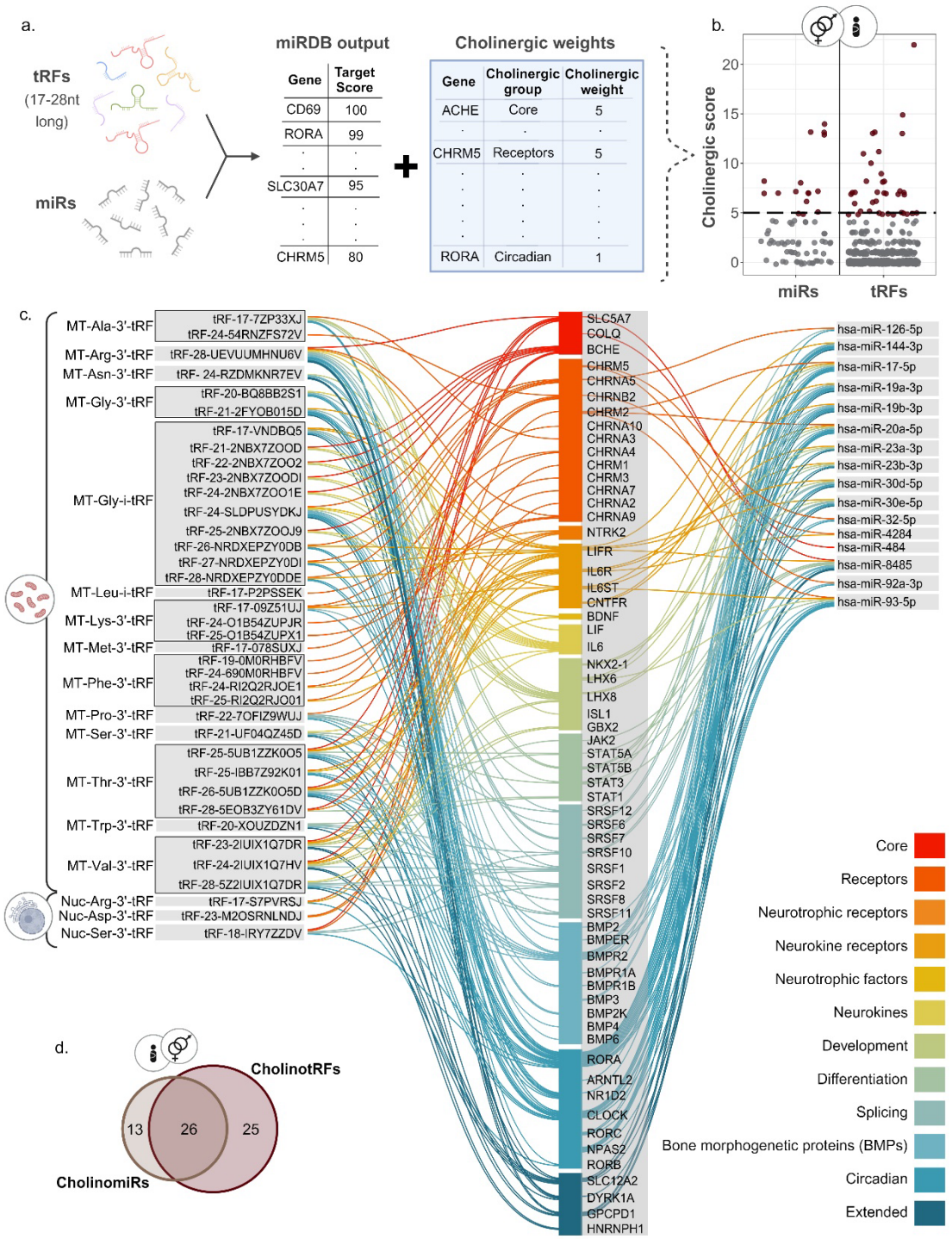

Figure 6 – CholinotRFs and CholinomiRs are predicted to target specific genes in the cholinergic system. (a) Combining the miRDB sequence-based prediction algorithm with our in-house cholinergic scoring system revealed 16 CholinomiRs and 38 CholinotRFs expressed in newborns. (b) Dot plot showing cholinergic score distribution across UCS miRs and tRFs in both male and female newborns. (c) Network plot presenting predicted targets of the newborn CholinomiRs (right-hand list), and CholinotRFs which are grouped according to their tRF families (left-hand list). tRF families with more than one cholinergic member are framed by black lines. The central list of 51 cholinergic genes that are predicted targets to the Cholino-miRs/tRFs is colored according to their gene sub-group within the cholinergic pathway. (d) Venn plot presenting the number of cholinergic gene targets shared between the newborn CholinomiRs and CholinotRFs. Created with BioRender.

4.7 tRF groups classify newborns according to PPS

To test whether short noncoding RNA levels may classify newborns into stress and control groups, we applied SVM Kernel classification with "leave-one-out" cross-validation to different sets of tRFs and miRs, testing the male and female groups together and apart, and seeking the best group of markers for this task (Supplementary table 9). Expectedly, the best classification was obtained for females, based on the levels of all of the seven UCS DE tRFs and the levels of the four female-specific UCS DE tRFs (Fig 7a, Supplementary table 10), with area under the ROC curve of 100% (AUC; 10,000 permutations, FDR ≤ 0.0001) and 98% respectively (FDR = 0.008). Interestingly, the next best classification in female newborns was achieved using the 38 CholinotRFs, yielding AUC of 95% (FDR = 0.008). In comparison, CholinomiRs reached an AUC of 88% (FDR = 0.051). Male newborns, however, yielded very low classification scores, all under chance levels (Figure 7d). When comparing males and females together, testing stress vs. control groups without accounting for sex (Figure 7b) achieved classification results that were a direct combination of the male and female separate classifications, with the best classification achieved by all of the UCS DE tRFs (AUC = 78%, FDR = 0.029). Taking into account sex as well (Figure 7c) achieved much better classification, with the lead marker groups still being the UCS DE tRFs (AUC: Female DE tRFs = 94%, FDR = 0.008; all DE tRFs = 93%, FDR = 0.008). These results further strengthen the perceived connection of these cholinergic tRFs to stress and its sex-specific effects.

Interestingly, combining our results with the previously published Fetal stress index (FSI) from the FELICITy cohort, a measurement of the fetus heart rate reactivity measured non-invasively during the third trimester (46) elevated some of the classification results (Supplementary Figure 8a-c, Supplementary table 9), although it was not correlated with any of the tRFs or miRs and by itself did not yield more than 48% AUC. This was especially the case in male newborns, where combination of the FSI and all four DE miRs from UCS and maternal serum achieved an AUC of 95% (FDR = 0.058; Supplementary Figure 8g, Supplementary table 10), an elevation of approximately 60%. In females, CholinotRFs together with FSI had an increase of 5%, reaching an AUC of 100% (FDR = 0.008; Supplementary Figure 8d, Supplementary table 10). A similar elevation was observed when separating stress and control groups of males and females together, with the combination of FSI and all DE tRFs yielding an AUC of 83% (FDR = 0.029, 5% elevation, Supplementary Figure 8e, Supplementary table 10). Most of the other marker sets did not do so well with the addition of FSI, showing decrease in classification success (Supplementary table 9). Together, these findings indicate that newborns can be differentiated by their mothers' PPS already at birth, as reflected by UCS short noncoding

RNAs, with the sex of the newborn playing a significant role in determining the type of markers required.

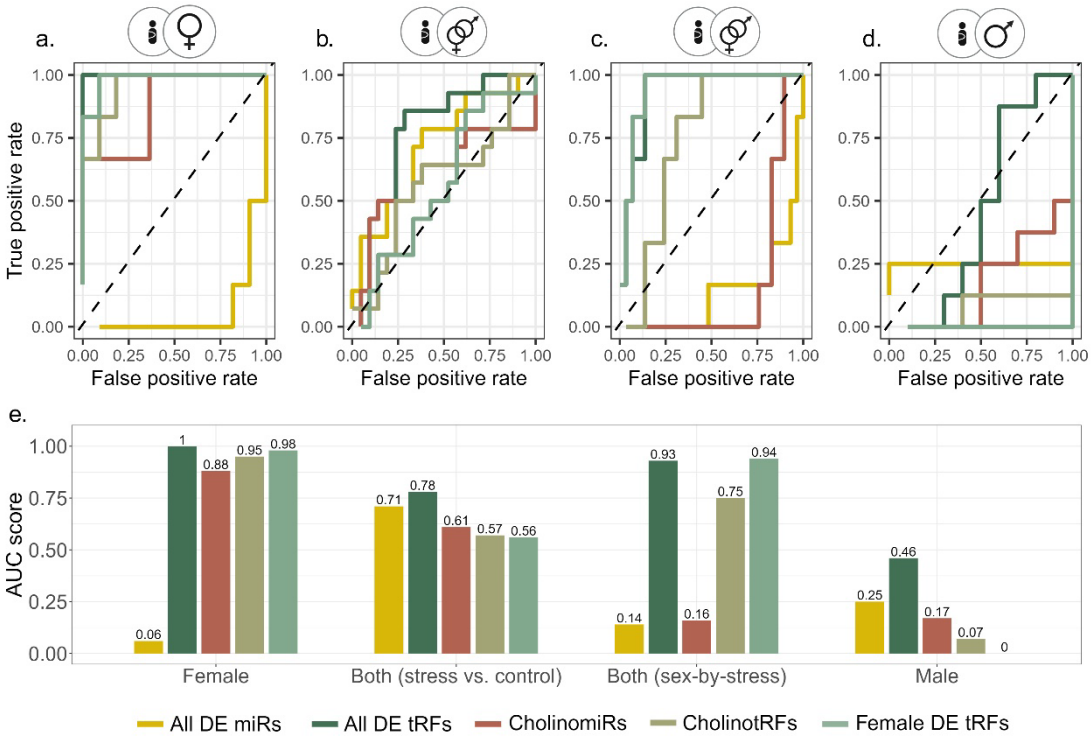

Figure 7 – CholinotRFs classify female newborns according to maternal PPS. (a-d) ROC curves of five marker groups (All DE tRFs, Female DE tRFs, CholinotRFs, All DE miRs, and CholinomiRs), classifying newborns to stress and control groups based on SVM Kernel algorithm with "leave one out" cross validation: (a) females (n= 6 vs. 11), (b) males & females (stress vs. control; n= 14 vs. 21), (c) males & females (stress-by-sex; n= 14 vs. 21), and (d) males (n= 8 vs. 10). (e) Bar plot of AUC values across comparisons with FDR based on 10,000 permutations (available in Supplementary table 9). Created with BioRender.

5 Discussion

Maternal PPS has long been known to affect the fetus (8–10, 12–17), but validated biomarkers for this phenomenon remained lacking. Here, we present a new group of biomarkers that reflect maternal PPS influence on the newborn. Specifically, we used maternal serum and UCS to differentiate participants into stress and control groups based on tRF expression patterns and ChE activity levels. We have also shown that these tRFs can be assigned to families according to their genome origin, cleavage type, and coded amino acid. These families, in turn, shared expression and length patterns that were specific not only to the differences between mothers and newborns, but also between sex and stress conditions, with the strongest effects observed in female newborns of PPS-affected mothers. We further identified possible cholinergic involvement by the discovery of higher AChE activity in the UCS of stressed newborns, with a stronger effect observed in males. Further, we found enrichment of

CholinomiRs and CholinotRFs in general, with the latter being able to classify the female newborns into stress and control groups with an AUC of 95%.

Our findings have a dual value. First and foremost, we have introduced a novel method for interpreting tRF sequencing results. Although sets of tRFs share many characteristics that warrant their assembly into groups, they are still perceived by the scientific community as separate entities. Thus, while the literature often mentions tRFs by their "family name" (MT i-tRF^{HisGTG}, Glu-50tsRNA-CTC, etc.) (99, 100), they are still referred to as single tRF molecules. In contradistinction, our classification into "tRF families" based on a combination of their genome origin, cleavage type and coded amino acid, has highlighted expression and length patterns that are context-specific, i.e., influenced by stress and sex. Furthermore, previous studies have identified "tRF storms", characterized by rising levels of tRFs that replaced miRs two days post-stroke (31). This marks the importance of mass production of tRFs (26), and strengthens the concept of a role for tRFs as a group rather than as individuals. With that in mind, we stress the importance of previous reports establishing specific functions of single tRFs in many diseases and conditions (27, 29–32, 34). We urge future researchers to take both these points into account when studying tRFs and to look for single and familial tRF functions.

To the best of our knowledge, three similar studies have been published. The first, by Akins et al. (101), examined multiple datasets seeking 5'-halfs and long 5'-tRFs in human patients and cell lines. They showed that while context-dependent, tRFs that share length and parental tRNA may also share expression levels and sequence. However, their DE analysis did not examine tRF families as groups directly, and their focus was on 5' -tRFs and -halves of very specific lengths, 27-41nt, which were almost completely absent in our data. A second study by Su et al. (33) investigated the influence of prenatal maternal immune activation in mice on tRFs in several tissues. Immune activation was performed at E11.5 and E12.5 and within a few hours after the second activation they thoroughly investigated the tRF landscape, including characterizing the length distribution according to cleavage type by both sequencing and northern blot analyses of tRFs grouped by their parental tRNAs. However, using STAR alignment (102) rather than the standard annotations of tRFs, rendered their analysis less translatable by the standard tools of the field. The third study, by Isakova et al. (103), presented a complex analysis, producing an atlas of short noncoding RNAs in different murine tissues. tRFs were only one part of this unique paper, and were aligned with a combination of STAR and Unitas (104). The authors looked at the sum of tRFs within each group as indicated by a combination of genome origin, cleavage type, coded amino acid and codon, and showed tissue-specific expression. However, they did not show the variability within the tRF groups,

and their only statistic for assessing them as groups was the sum of expression. In addition, i-tRFs were absent from their analysis. Thus, all three papers retained groupings based on single amino acid codons, while we have introduced the use of the binomial test as an innovative analysis that showed tRF families working as groups. Each tRF family shared common expression patterns and length distributions, as well as sequence similarities, even within the wider boundaries of a single amino acid rather than a single codon.

The second novel point we present in our study is the usage of tRFs as biomarkers, differentiating the newborns according to maternal stress and enabling classification of newborns by sex. We discovered stress-specific tRF patterns, with the leading effect consisting of a major decrease in MT tRFs. This effect appeared in both sexes, but was stronger in female newborns. Although our cohort is unique, it is small, including only 35 sequenced samples, and due to low RNA quantities, we were not able to validate our findings by qPCR measurements in the rest of the cohort. Furthermore, we did not find publicly available datasets that were similar enough by tissue and species to validate our results, most likely due to the complexity of generating a similar cohort. However, previous animal studies show similar effects: Bartho et al. (105) revealed that cortisone injected to pregnant mice between E12.5 and E14.5 produced a decrease in mitochondrial DNA in the placenta of female compared to male offspring, and Su et al. (33) showed that the overall percentage of MT tRFs in a murine prenatal immune activation model was significantly higher in the fetal brain and liver of females compared to those of males.

The magnitude of the MT tRF effect can also be explained by the fact that we used serum rather than whole blood or PBMCs. RNA in the serum reflects the content of extracellular vesicles and all broken blood cells, including platelets which are rich in mitochondria (106). Although serum RNA amounts are low (107), it is the standard blood fraction in use in hospital settings and therefore forms an available pool for RNA-seq clinical studies. And although this sequencing requires more specialized library preparation kits, the resulting enrichment in short RNAs (107, 108) compensates for their low yield.

Importantly, serum is also a standard tissue for measuring cholinergic tone, defined as the balance between AChE and BChE, both of which hydrolyze acetylcholine to acetate and choline. AChE acts as the main cholinesterase of the central nervous system and BChE of the periphery (35, 36). In the fetal environment, besides the erythrocyte-bound blood AChE (41), the enzyme is found in the placenta and in umbilical cord endothelial cells (109, 110). Indeed, we found higher AChE levels in the UCS compared to the maternal serum, followed by stress-

related elevation in newborns. This effect was more predominant in male compared to female newborns, in line with previous work showing larger stress-related differences in male newborns (9, 18, 45). By hydrolyzing acetylcholine, the two ChEs can reduce its anti-inflammatory effect, indirectly activating pro-inflammatory pathways. These include the NF-κB pathway which contradicts the vagus-mediated acetylcholine secretion in response to an activated HPA (36, 37, 111). This process is also regulated by short noncoding RNAs (41, 111), compatible with our findings of enriched CholinotRFs and CholinomiRs, albeit without direct connection between the short noncoding Cholino-RNAs and the two ChEs in our data. Notably, transgenic excess of the AChE-targeting CholinomiR miR-132 was shown to be incompatible with fetal survival in mice (112). Furthermore, mice show direct cholinergic influence of prenatal stress, where both physical and psychological stress were connected to anxiety-like behaviors and memory impairment that could be caused by hyperexcitability of the cholinergic neurons in the latero-dorsal tegmentum (113). However, that experiment was performed only on male offspring, to avoid the effect of “hormonal interference” that was observed in previous studies (114–116).

In summary, our study has demonstrated the importance of tRF families as biomarkers that reflect the effect of maternal PPS on newborns, as early as the birth itself. We have presented a new type of analysis that takes into consideration the function of families of tRFs, rather than single tRFs, as determined by their genome origin, cleavage type, and coded amino acid. We have shown the involvement in this phenomenon of the cholinergic system, by both ChE activities, and CholinomiR and CholinotRF small non-coding RNAs. We believe that these findings play an important role in early diagnosis of stress effects in newborns and encourage further research into the landscape of tRFs in prenatal and other stress-related conditions.

6 Acknowledgements

The authors wish to thank all participants and all the medical staff at the labor and delivery of the Department of Obstetrics and Gynecology (Klinikum rechts der Isar, Technical University of Munich, Germany) for their valuable contribution to the study.

7 Funding

The research leading to these results received funding from the Israel Science Foundation, ISF (835/23; to H.S.), and from a joint research support to H.S. and L.C. from The Hebrew

University. We further acknowledge Ken Stein and Keter Holdings support. L.C. is the Snyder Granadar chair in Genetics, H.S. is the Slesinger chair in Molecular Neuroscience. In addition, this work was supported by a Hans Fischer Senior Fellowship from IAS-TUM (Institute for Advanced Study - Technical University of Munich, Munich, Germany) awarded to M.C.A., as well as funds from the Department of Obstetrics and Gynecology, Klinikum rechts der Isar, Technical University of Munich, Germany to S.M.L., and CIHR to M.G.F. (grant number 123489).

8 Conflict of interest statement

None declared.

9 Ethics approval

The study protocol is in strict accordance with the Committee of Ethical Principles for Medical Research from TUM and has the approval of the 'Ethikkommission der Fakultat fur Medizin der Technische Universitat Munchen' (registration number 151/16S). ClinicalTrials.gov registration number is NCT03389178. Written informed consent was received from participants prior to inclusion in the study.

10 References

1. Lugo-Candelas,C., Hwei,T., Lee,S., Lucchini,M., Smaniotto Aizza,A., Kahn,L.G., Buss,C., O'Connor,T.G., Ghassabian,A., Padula,A.M., *et al.* (2023) Prenatal sleep health and risk of offspring ADHD symptomatology and associated phenotypes: a prospective analysis of timing and sex differences in the ECHO cohort. *The Lancet Regional Health - Americas*, **27**, 100609.

2. Trowbridge,J., Abrahamsson,D., Bland,G.D., Jiang,T., Wang,M., Park,J.-S., Morello-Frosch,R., Sirota,M., Lee,H., Goin,D.E., *et al.* (2023) Extending Nontargeted Discovery of Environmental Chemical Exposures during Pregnancy and Their Association with Pregnancy Complications—A Cross-Sectional Study. *Environ Health Perspect*, **131**.

3. Bakhireva,L.N., Solomon,E., Roberts,M.H., Ma,X., Rai,R., Wiesel,A., Jacobson,S.W., Weinberg,J. and Milligan,E.D. (2024) Independent and Combined Effects of Prenatal Alcohol Exposure and Prenatal Stress on Fetal HPA Axis Development. *Int J Mol Sci*, **25**, 2690.

4. Vinnars,M.T., Bixo,M. and Damdimopoulou,P. (2023) Pregnancy-related maternal physiological adaptations and fetal chemical exposure. *Mol Cell Endocrinol*, **578**.

5. Sinha,T., Brushett,S., Prins,J. and Zhernakova,A. (2023) The maternal gut microbiome during pregnancy and its role in maternal and infant health. *Curr Opin Microbiol*, **74**.

6. Muglia,L.J., Benhalima,K., Tong,S. and Ozanne,S. (2022) Maternal factors during pregnancy influencing maternal, fetal, and childhood outcomes. *BMC Med*, **20**.

7. Kumar,D., Verma,S. and Mysorekar,I.U. (2023) COVID-19 and pregnancy: clinical outcomes; mechanisms, and vaccine efficacy. *Translational Research*, **251**, 84–95.

8. Wu,Y., Espinosa,K.M., Barnett,S.D., Kapse,A., Quistorff,J.L., Lopez,C., Andescavage,N., Pradhan,S., Lu,Y.-C., Kapse,K., *et al.* (2022) Association of Elevated Maternal Psychological Distress, Altered Fetal Brain, and Offspring Cognitive and Social-Emotional Outcomes at 18 Months. *JAMA Netw Open*, **5**, e229244.

9. Walsh,K., McCormack,C.A., Webster,R., Pinto,A., Lee,S., Feng,T., Krakovsky,H.S., O'Grady,S.M., Tycko,B., Champagne,F.A., *et al.* (2019) Maternal prenatal stress phenotypes associate with fetal neurodevelopment and birth outcomes. *Proceedings of the National Academy of Sciences*, **116**, 23996–24005.

10. Schalla,MA. and Stengel,A. (2024) The role of stress in perinatal depression and anxiety – A systematic review. *Front Neuroendocrinol*, **72**, 101117.

11. Cohen,S., Kamarck,T. and Mermelstein,R. (1983) A Global Measure of Perceived Stress. *J Health Soc Behav*, **24**, 385.

12. Graham,A.M., Doyle,O., Tilden,E.L., Sullivan,E.L., Gustafsson,H.C., Marr,M., Allen,M. and Mackiewicz Seghete,K.L. (2022) Effects of Maternal Psychological Stress During Pregnancy on Offspring Brain Development: Considering the Role of Inflammation and Potential for Preventive Intervention. *Biol Psychiatry Cogn Neurosci Neuroimaging*, **7**, 461–470.

13. Dhaliwal,S.K., Dabelea,D., Lee-Winn,A.E., Crume,T., Wilkening,G. and Perng,W. (2023) Maternal psychosocial stress during pregnancy and offspring neurobehavioral outcomes during early childhood in the Healthy Start Study. *Ann Epidemiol*, **86**, 16-24.e3.

14. Wu,Y., Lu,Y.-C., Jacobs,M., Pradhan,S., Kapse,K., Zhao,L., Niforatos-Andescavage,N., Vezina,G., du Plessis,A.J. and Limperopoulos,C. (2020) Association of Prenatal Maternal Psychological Distress With Fetal Brain Growth, Metabolism, and Cortical Maturation. *JAMA Netw Open*, **3**, e1919940.

15. Moog,N.K., Nolvi,S., Kleih,T.S., Styner,M., Gilmore,J.H., Rasmussen,J.M., Heim,C.M., Entringer,S., Wadhwa,P.D. and Buss,C. (2021) Prospective association of maternal psychosocial stress in pregnancy with newborn hippocampal volume and implications for infant social-emotional development. *Neurobiol Stress*, **15**, 100368.

16. Moshfeghinia,R., Torabi,A., Mostafavi,S., Rahbar,S., Moradi,M.S., Sadeghi,E., Mootz,J. and Vardanjani,H.M. (2023) Maternal psychological stress during pregnancy and newborn telomere length: a systematic review and meta-analysis. *BMC Psychiatry*, **23**, 947.

17. Entringer,S., Epel,E.S., Lin,J., Buss,C., Shahbaba,B., Blackburn,E.H., Simhan,H.N. and Wadhwa,P.D. (2013) Maternal psychosocial stress during pregnancy is associated with newborn leukocyte telomere length. *Am J Obstet Gynecol*, **208**, 134.e1-134.e7.

18. Lehtola,S.J., Tuulari,J.J., Scheinin,N.M., Karlsson,L., Parkkola,R., Merisaari,H., Lewis,J.D., Fonov,V.S., Louis Collins,D., Evans,A., *et al.* (2020) Newborn amygdalar volumes are associated with maternal prenatal psychological distress in a sex-dependent way. *Neuroimage Clin*, **28**, 102380.

19. Cao-Lei,L., de Rooij,S.R., King,S., Matthews,S.G., Metz,G.A.S., Roseboom,T.J. and Szyf,M. (2020) Prenatal stress and epigenetics. *Neurosci Biobehav Rev*, **117**, 198–210.

20. Hantsoo,L., Kornfield,S., Anguera,M.C. and Epperson,C.N. (2019) Inflammation: A Proposed Intermediary Between Maternal Stress and Offspring Neuropsychiatric Risk. *Biol Psychiatry*, **85**, 97–106.

21. Vuppaladhadiam,L., Lager,J., Fiehn,O., Weiss,S., Chesney,M., Hasdemir,B. and Bhargava,A. (2021) Human Placenta Buffers the Fetus from Adverse Effects of Perceived Maternal Stress. *Cells*, **10**, 379.

22. Chen,Q., Zhang,X., Shi,J., Yan,M. and Zhou,T. (2021) Origins and evolving functionalities of tRNA-derived small RNAs. *Trends Biochem Sci*, **46**, 790–804.

23. Kuhle,B., Chen,Q. and Schimmel,P. (2023) tRNA renovatio: Rebirth through fragmentation. *Mol Cell*, **83**, 3953–3971.

24. Magee,R. and Rigoutsos,I. (2020) On the expanding roles of tRNA fragments in modulating cell behavior. *Nucleic Acids Res*, **48**, 9433–9448.

25. Telonis,A.G., Kirino,Y. and Rigoutsos,I. (2015) Mitochondrial tRNA-lookalikes in nuclear chromosomes: Could they be functional? *RNA Biol*, **12**, 375–380.

26. Yu,X., Xie,Y., Zhang,S., Song,X., Xiao,B. and Yan,Z. (2021) tRNA-derived fragments: Mechanisms underlying their regulation of gene expression and potential applications as therapeutic targets in cancers and virus infections. *Theranostics*, **11**, 461–469.

27. Fu,M., Gu,J., Wang,M., Zhang,J., Chen,Y., Jiang,P., Zhu,T. and Zhang,X. (2023) Emerging roles of tRNA-derived fragments in cancer. *Mol Cancer*, **22**, 30.

28. Su,Z., Wilson,B., Kumar,P. and Dutta,A. (2020) Noncanonical Roles of tRNAs: tRNA Fragments and Beyond. *Annu Rev Genet*, **54**, 47–69.

29. Shulman,D., Dubnov,S., Zorbaz,T., Madrer,N., Paldor,I., Bennett,D.A., Seshadri,S., Mufson,E.J., Greenberg,D.S., Loewenstein,Y., *et al.* (2023) Sex-specific declines in cholinergic-targeting tRNA fragments in the nucleus accumbens in Alzheimer's disease. *Alzheimer's & Dementia*, **19**, 5159–5172.

30. Paldor,I., Madrer,N., Vaknine Treidel,S., Shulman,D., Greenberg,D.S. and Soreq,H. (2022) Cerebrospinal fluid and blood profiles of transfer RNA fragments show age, sex, and Parkinson's disease-related changes. *J Neurochem*, 10.1111/jnc.15723.

31. Winek,K., Lobentanzer,S., Nadorp,B., Dubnov,S., Dames,C., Jagdmann,S., Moshitzky,G., Hotter,B., Meisel,C., Greenberg,D.S., *et al.* (2020) Transfer RNA fragments replace microRNA regulators of the cholinergic poststroke immune blockade. *Proc Natl Acad Sci U S A*, **117**, 32606–32616.

32. Tzur,Y., Winek,K., Madrer,N., Dubnov,S., Bennett,E.R., Greenberg,D.S., Hanin,G., Gammal,A., Tam,J., Arkin,I.T., *et al.* (2024) Lysine tRNA fragments and miR-194-5p co-regulate hepatic steatosis via β-Klotho and perilipin 2. *Mol Metab*, **79**, 101856.

33. Su,Z., Frost,E.L., Lammert,C.R., Przanowska,R.K., Lukens,J.R. and Dutta,A. (2020) tRNA-derived fragments and microRNAs in the maternal-fetal interface of a mouse maternal-immune-activation autism model. *RNA Biol*, **17**, 1183–1195.

34. Cooke,W.R., Jiang,P., Ji,L., Bai,J., Jones,G.D., Lo,Y.M.D., Redman,C. and Vatish,M. (2024) Differential 5′-tRNA Fragment Expression in Circulating Preeclampsia Syncytiotrophoblast Vesicles Drives Macrophage Inflammation. *Hypertension*, **81**, 876–886.

35. Soreq,H. (2015) Checks and balances on cholinergic signaling in brain and body function. *Trends Neurosci*, **38**, 448–458.

36. Vaknine,S. and Soreq,H. (2020) Central and peripheral anti-inflammatory effects of acetylcholinesterase inhibitors. *Neuropharmacology*, **168**, 108020.

37. Cerritelli,F., Frasch,M.G., Antonelli,M.C., Viglione,C., Vecchi,S., Chiera,M. and Manzotti,A. (2021) A Review on the Vagus Nerve and Autonomic Nervous System During Fetal Development: Searching for Critical Windows. *Front Neurosci*, **15**, 1184.

38. Shenhar-Tsarfaty,S., Berliner,S., Bornstein,N.M. and Soreq,H. (2014) Cholinesterases as biomarkers for parasympathetic dysfunction and inflammation-related disease. *Journal of Molecular Neuroscience*, **53**, 298–305.

39. Winek,K., Soreq,H. and Meisel,A. (2021) Regulators of cholinergic signaling in disorders of the central nervous system. *J Neurochem*, **00**, jnc.15332.

40. Nadorp,B. and Soreq,H. (2014) Predicted overlapping microRNA regulators of acetylcholine packaging and degradation in neuroinflammation-related disorders. *Front Mol Neurosci*, **7**, 9.

41. Madrer,N. and Soreq,H. (2020) Cholino-ncRNAs modulate sex-specific- and age-related acetylcholine signals. *FEBS Lett*, **594**, 2185–2198.

42. Lobentanzer,S., Hanin,G., Klein,J. and Soreq,H. (2019) Integrative Transcriptomics Reveals Sexually Dimorphic Control of the Cholinergic/Neurokine Interface in Schizophrenia and Bipolar Disorder. *Cell Rep*, **29**, 764-777.e5.

43. Antonelli,M.C., Frasch,M.G., Rumi,M., Sharma,R., Zimmermann,P., Molinet,M.S. and Lobmaier,S.M. (2022) Early Biomarkers and Intervention Programs for the Infant Exposed to Prenatal Stress. *Curr Neuropharmacol*, **20**, 94–106.

44. Sharma,R., Frasch,M.G., Zelgert,C., Zimmermann,P., Fabre,B., Wilson,R., Waldenberger,M., MacDonald,J.W., Bammler,T.K., Lobmaier,S.M., *et al.* (2022) Maternal–fetal stress and DNA methylation signatures in neonatal saliva: an epigenome-wide association study. *Clin Epigenetics*, **14**.

45. Zimmermann,P., Antonelli,M.C., Sharma,R., Müller,A., Zelgert,C., Fabre,B., Wenzel,N., Wu,H.-T., Frasch,M.G. and Lobmaier,S.M. (2022) Prenatal stress perturbs fetal iron homeostasis in a sex specific manner. *Sci Rep*, **12**, 9341.

46. Lobmaier,S.M., Müller,A., Zelgert,C., Shen,C., Su,P.C., Schmidt,G., Haller,B., Berg,G., Fabre,B., Weyrich,J., *et al.* (2020) Fetal heart rate variability responsiveness to maternal stress, non-invasively detected from maternal transabdominal ECG. *Arch Gynecol Obstet*, **301**, 405–414.

47. Alderdice,F. and Lynn,F. (2011) Factor structure of the Prenatal Distress Questionnaire. *Midwifery*, **27**, 553–559.

48. Pös,O., Biró,O., Szemes,T. and Nagy,B. (2018) Circulating cell-free nucleic acids: Characteristics and applications. *European Journal of Human Genetics*, **26**, 937–945.

49. Andrews,S. (2010) FastQC a quality control tool for high throughput sequence data.

50. Martin,M. (2011) Cutadapt removes adapter sequences from high-throughput sequencing reads. *EMBnet J*, **17**, 10–12.

51. Dodt,M., Roehr,J.T., Ahmed,R. and Dieterich,C. (2012) FLEXBAR-Flexible Barcode and Adapter Processing for Next-Generation Sequencing Platforms. *Biology (Basel)*, **1**, 895–905.

52. Roehr,J.T., Dieterich,C. and Reinert,K. (2017) Flexbar 3.0 - SIMD and multicore parallelization. *Bioinformatics*, **33**, 2941–2942.

53. Loher,P., Telonis,A.G. and Rigoutsos,I. (2017) MINTmap: fast and exhaustive profiling of nuclear and mitochondrial tRNA fragments from short RNA-seq data. *Sci Rep*, **7**, 41184.

54. Pliatsika,V., Loher,P., Telonis,A.G. and Rigoutsos,I. (2016) MINTbase: A framework for the interactive exploration of mitochondrial and nuclear tRNA fragments. *Bioinformatics*, **32**, 2481–2489.

55. Friedländer,M.R., MacKowiak,S.D., Li,N., Chen,W. and Rajewsky,N. (2012) MiRDeep2 accurately identifies known and hundreds of novel microRNA genes in seven animal clades. *Nucleic Acids Res*, **40**, 37–52.

56. Griffiths-Jones,S. (2004) The microRNA Registry. *Nucleic Acids Res*, **32**, 109D – 111.

57. Griffiths-Jones,S. (2006) miRBase: microRNA sequences, targets and gene nomenclature. *Nucleic Acids Res*, **34**, D140–D144.

58. Kozomara,A. and Griffiths-Jones,S. (2014) miRBase: annotating high confidence microRNAs using deep sequencing data. *Nucleic Acids Res*, **42**, D68–D73.

59. Kozomara,A. and Griffiths-Jones,S. (2011) miRBase: integrating microRNA annotation and deep-sequencing data. *Nucleic Acids Res*, **39**, D152–D157.

60. Kozomara,A., Birgaoanu,M. and Griffiths-Jones,S. (2019) miRBase: from microRNA sequences to function. *Nucleic Acids Res*, **47**, D155–D162.

61. Griffiths-Jones,S., Saini,H.K., van Dongen,S. and Enright,A.J. (2007) miRBase: tools for microRNA genomics. *Nucleic Acids Res*, **36**, D154–D158.

62. Bodenhofer,U., Bonatesta,E., Horejš-Kainrath,C. and Hochreiter,S. (2015) msa: an R package for multiple sequence alignment. *Bioinformatics*, **31**, 3997–3999.

63. Suzuki,T., Yashiro,Y., Kikuchi,I., Ishigami,Y., Saito,H., Matsuzawa,I., Okada,S., Mito,M., Iwasaki,S., Ma,D., *et al.* (2020) Complete chemical structures of human mitochondrial tRNAs. *Nat Commun*, **11**.

64. Ellman,G.L., Courtney,K.D., Andres,V. and Featherstone,R.M. (1961) A new and rapid colorimetric determination of acetylcholinesterase activity. *Biochem Pharmacol*, **7**, 88–95.

65. R Core Team (2019) R: A Language and Environment for Statistical Computing.

66. Love,M.I., Huber,W. and Anders,S. (2014) Moderated estimation of fold change and dispersion for RNA-seq data with DESeq2. *Genome Biol*, **15**, 1–21.

67. Liu,W. and Wang,X. (2019) Prediction of functional microRNA targets by integrative modeling of microRNA binding and target expression data. *Genome Biol*, **20**, 1–10.

68. Chen,Y. and Wang,X. (2020) miRDB: an online database for prediction of functional microRNA targets. *Nucleic Acids Res*, **48**, D127–D131.

69. Kuhn,M. (2022) caret: Classification and Regression Training.

70. John,C.R. (2020) MLeval: Machine learning model evaluation.

71. Chan,P.P. and Lowe,T.M. (2009) GtRNAdb: A database of transfer RNA genes detected in genomic sequence. *Nucleic Acids Res*, **37**, 93–97.

72. Chan,P.P. and Lowe,T.M. (2016) GtRNAdb 2.0: an expanded database of transfer RNA genes identified in complete and draft genomes. *Nucleic Acids Res*, **44**, D184–D189.

73. Juhling,F., Morl,M., Hartmann,R.K., Sprinzl,M., Stadler,P.F. and Putz,J. (2009) tRNAdb 2009: compilation of tRNA sequences and tRNA genes. *Nucleic Acids Res*, **37**, D159–D162.

74. Tan,H.C., Hsu,J.W., Tai,E.S., Chacko,S., Wu,V., Lee,C.F., Kovalik,J.P. and Jahoor,F. (2022) De Novo Glycine Synthesis Is Reduced in Adults With Morbid Obesity and Increases Following Bariatric Surgery. *Front Endocrinol (Lausanne)*, **13**.

75. Alves,A., Bassot,A., Bulteau,A.L., Pirola,L. and Morio,B. (2019) Glycine metabolism and its alterations in obesity and metabolic diseases. *Nutrients*, **11**.

76. Imenshahidi,M. and Hossenzadeh,H. (2022) Effects of glycine on metabolic syndrome components: a review. *J Endocrinol Invest*, **45**, 927–939.

77. Rasmussen,B.F., Ennis,M.A., Dyer,R.A., Lim,K. and Elango,R. (2021) Glycine, a Dispensable Amino Acid, Is Conditionally Indispensable in Late Stages of Human Pregnancy. *Journal of Nutrition*, **151**, 361–369.

78. Chen,F., Song,C., Meng,F., Zhu,Y., Chen,X., Fang,X., Ma,D., Wang,Y. and Zhang,C. (2023) 5'-tRF-GlyGCC promotes breast cancer metastasis by increasing fat mass and obesity-associated protein demethylase activity. *Int J Biol Macromol*, **226**, 397–409.

79. Liao,T., Gan,M., Lei,Y., Wang,Y., Chen,L., Shen,L. and Zhu,L. (2023) Dynamic changes in the transcriptome of tRNA-derived small RNAs related with fat metabolism. *Sci Data*, **10**.

80. Barnett,M.M., Reay,W.R., Geaghan,M.P., Kiltschewskij,D.J., Green,M.J., Weidenhofer,J., Glatt,S.J. and Cairns,M.J. (2023) miRNA cargo in circulating vesicles from neurons is altered in individuals with schizophrenia and associated with severe disease.

81. Ripke,S., Sanders,A.R., Kendler,K.S., Levinson,D.F., Sklar,P., Holmans,P.A., Lin,D.Y., Duan,J., Ophoff,R.A., Andreassen,O.A., *et al.* (2011) Genome-wide association study identifies five new schizophrenia loci. *Nat Genet*, **43**, 969–978.

82. Håvik,B., Le Hellard,S., Rietschel,M., Lybæk,H., Djurovic,S., Mattheisen,M., Mhleisen,T.W., Degenhardt,F., Priebe,L., Maier,W., *et al.* (2011) The complement control-related genes CSMD1 and CSMD2 associate to schizophrenia. *Biol Psychiatry*, **70**, 35–42.

83. Liu,Y., Fu,X., Tang,Z., Li,C., Xu,Y., Zhang,F., Zhou,D. and Zhu,C. (2019) Altered expression of the CSMD1 gene in the peripheral blood of schizophrenia patients. *BMC Psychiatry*, **19**.

84. Selmaj,I., Cichalewska,M., Namiecinska,M., Galazka,G., Horzelski,W., Selmaj,K.W. and Mycko,M.P. (2017) Global exosome transcriptome profiling reveals biomarkers for multiple sclerosis. *Ann Neurol*, **81**, 703–717.

85. Flamant,S., Chomel,J.C., Desterke,C., Féraud,O., Gobbo,E., Mitjavila-Garcia,M.T., Foudi,A., Griscelli,F., Turhan,A.G. and Bennaceur-Griscelli,A. (2019) Global microRNA profiling uncovers miR-206 as a negative regulator of hematopoietic commitment in human pluripotent stem cells. *Int J Mol Sci*, **20**.

86. Mikulski,D., Nowicki,M., Dróżdż,I., Misiewicz,M., Kościelny,K.P., Okoński,K., Krawiec,K., Perdas,E., Wierzbowska,A. and Fendler,W. (2023) High serum miR-223-3p expression level predicts complete response and prolonged overall survival in multiple myeloma patients undergoing autologous hematopoietic stem cell transplantation. *Front Oncol*, **13**.

87. Su,S., Zhao,Q., He,C., Huang,D., Liu,J., Chen,F., Chen,J., Liao,J.Y., Cui,X., Zeng,Y., *et al.* (2015) miR-142-5p and miR-130a-3p are regulated by IL-4 and IL-13 and control profibrogenic macrophage program. *Nat Commun*, **6**.

88. Liao,R., Sun,J., Zhang,L., Lou,G., Chen,M., Zhou,D., Chen,Z. and Zhang,S. (2008) MicroRNAs play a role in the development of human hematopoietic stem cells. *J Cell Biochem*, **104**, 805–817.

89. Kim,B.S., Jung,J.Y., Jeon,J.Y., Kim,H.A. and Suh,C.H. (2016) Circulating hsa-miR-30e-5p, hsa-miR-92a-3p, and hsa-miR-223-3p may be novel biomarkers in systemic lupus erythematosus. *HLA*, **88**, 187–193.

90. Ma,F., Chen,D., Chi,Y., Chen,F., Li,X. and Han,Z. (2013) The expression and role of miR-301a in human umbilical cord-derived mesenchymal stromal cells. *Cytotherapy*, **15**, 1511–1516.

91. Granda-Díaz,R., Manterola,L., Hermida-Prado,F., Rodríguez,R., Santos,L., García-de-la-Fuente,V., Fernández,M.T., Corte-Torres,M.D., Rodrigo,J.P., Álvarez-Teijeiro,S., *et al.* (2023) Targeting oncogenic functions of miR-301a in head and neck squamous cell carcinoma by PI3K/PTEN and MEK/ERK pathways. *Biomedicine and Pharmacotherapy*, **161**.

92. Fernández-Pato,A., Virseda-Berdices,A., Resino,S., Ryan,P., Martínez-González,O., Pérez-García,F., Martin-Vicente,M., Valle-Millares,D., Brochado-Kith,O., Blancas,R., *et al.* (2022) Plasma miRNA profile at COVID-19 onset predicts severity status and mortality. *Emerg Microbes Infect*, **11**, 676–688.

93. Seong,R.K., Lee,J.K., Cho,G.J., Kumar,M. and Shin,O.S. (2020) mRNA and miRNA profiling of Zika virus-infected human umbilical cord mesenchymal stem cells identifies miR-142-5p as an antiviral factor. *Emerg Microbes Infect*, **9**, 2061–2075.

94. Hamza,S., Garanina,E.E., Shkair,L., Alsaadi,M., Khaiboullina,S.F. and Tezcan,G. (2024) Implications of NLRP3 Suppression Using Glibenclamide and miR-223 against Colorectal Cancer. *Pharmaceuticals*, **17**, 299.

95. Stverakova,T., Baranova,I., Mikyskova,P., Gajdosova,B., Vosmikova,H., Laco,J., Palicka,V. and Parova,H. (2023) Selection of endogenous control and identification of significant microRNA deregulations in cervical cancer. *Front Oncol*, **13**.

96. Zhang,X., Yan,Z., Zhang,J., Gong,L., Li,W., Cui,J., Liu,Y., Gao,Z., Li,J., Shen,L., *et al.* (2011) Combination of hsa-miR-375 and hsa-miR-142-5p as a predictor for recurrence risk in gastric cancer patients following surgical resection. *Annals of Oncology*, **22**, 2257–2266.

97. Pillay,P., Moodley,K., Vatish,M. and Moodley,J. (2020) Exosomal microRNAs in pregnancy provides insight into a possible cure for cancer. *Int J Mol Sci*, **21**, 1–16.

98. Gu,H., Chen,L., Xue,J., Huang,T., Wei,X., Liu,D., Ma,W., Cao,S. and Yuan,Z. (2019) Expression profile of maternal circulating microRNAs as non-invasive biomarkers for

prenatal diagnosis of congenital heart defects. *Biomedicine and Pharmacotherapy*, **109**, 823–830.

99. Soureas,K., Papadimitriou,M., Malandrakis,P., Papanota,A., Adamopoulos,P.G., Ntanasis-Stathopoulos,I., Liacos,C., Gavriatopoulou,M., Sideris,D.C., Kastritis,E., *et al.* (2024) Small RNA-seq and clinical evaluation of tRNA-derived fragments in multiple myeloma: Loss of mitochondrial i-tRF HisGTG results in patients' poor treatment outcome. *Br J Haematol*, 10.1111/bjh.19332.

100. Li,D., Gao,X., Ma,X., Wang,M., Cheng,C., Xue,T., Gao,F., Shen,Y., Zhang,J. and Liu,Q. (2024) Aging-induced tRNAGlu-derived fragment impairs glutamate biosynthesis by targeting mitochondrial translation-dependent cristae organization. *Cell Metab*, 10.1016/j.cmet.2024.02.011.

101. Akins,R.B., Ostberg,K., Cherlin,T., Tsiouplis,N.J., Loher,P. and Rigoutsos,I. (2023) The Typical tRNA Co-Expresses Multiple 5' tRNA Halves Whose Sequences and Abundances Depend on Isodecoder and Isoacceptor and Change with Tissue Type, Cell Type, and Disease. *Noncoding RNA*, **9**, 69.

102. Dobin,A., Davis,C.A., Schlesinger,F., Drenkow,J., Zaleski,C., Jha,S., Batut,P., Chaisson,M. and Gingeras,T.R. (2013) STAR: Ultrafast universal RNA-seq aligner. *Bioinformatics*, **29**, 15–21.

103. Isakova,A., Fehlmann,T., Keller,A. and Quake,S.R. A mouse tissue atlas of small noncoding RNA. 10.1073/pnas.2002277117/-/DCSupplemental.

104. Gebert,D., Hewel,C. and Rosenkranz,D. (2017) Unitas: The universal tool for annotation of small RNAs. *BMC Genomics*, **18**.

105. Bartho,L.A., Holland,O.J., Moritz,K.M., Perkins,A. V. and Cuffe,J.S.M. (2019) Maternal corticosterone in the mouse alters oxidative stress markers, antioxidant function and mitochondrial content in placentas of female fetuses. *J Physiol*, **597**, 3053–3067.

106. Picard,M. (2021) Blood mitochondrial DNA copy number: What are we counting? *Mitochondrion*, **60**, 1–11.

107. Hulstaert,E., Morlion,A., Avila Cobos,F., Verniers,K., Nuytens,J., Vanden Eynde,E., Yigit,N., Anckaert,J., Geerts,A., Hindryckx,P., *et al.* (2020) Charting Extracellular Transcriptomes in The Human Biofluid RNA Atlas. *Cell Rep*, **33**.

108. Godoy,P.M., Bhakta,N.R., Barczak,A.J., Cakmak,H., Fisher,S., MacKenzie,T.C., Patel,T., Price,R.W., Smith,J.F., Woodruff,P.G., *et al.* (2018) Large Differences in Small RNA Composition Between Human Biofluids. *Cell Rep*, **25**, 1346–1358.

109. Carvalho,A.F., Graça,L.M., Martins-Silva,J. and Saldanha,C. (2005) Biochemical characterization of human umbilical vein endothelial cell membrane bound acetylcholinesterase. *FEBS Journal*, **272**, 5584–5594.

110. Ruma Sun-y,B. V (1997) Human Placentai Cholinergic System. *Biochem Pharmacol*, **53**, 1577–1586.

111. Zorbaz,T., Madrer,N. and Soreq,H. (2022) Cholinergic blockade of neuroinflammation: from tissue to RNA regulators. *Neuronal Signal*, **6**.

112. Hanin,G., Yayon,N., Tzur,Y., Haviv,R., Bennett,E.R., Udi,S., Krishnamoorthy,Y.R., Kotsiliti,E., Zangen,R., Efron,B., *et al.* (2018) miRNA-132 induces hepatic steatosis and hyperlipidaemia by synergistic multitarget suppression. *Gut*, **67**, 1124–1134.

113. Shabani,M., Ilaghi,M., Naderi,R. and Razavinasab,M. (2023) The hyperexcitability of laterodorsal tegmentum cholinergic neurons accompanies adverse behavioral and cognitive outcomes of prenatal stress. *Sci Rep*, **13**.

114. GhotbiRavandi,S., Shabani,M., Bakhshaei,S., Nazeri,M. and Nozari,M. (2021) Effects of psychological or physical prenatal stress on attention and locomotion in juvenile rats. *International Journal of Neuroscience*, **131**, 233–238.

115. Iturra-Mena,A.M., Arriagada-Solimano,M., Luttecke-Anders,A. and Dagnino-Subiabre,A. (2018) Effects of prenatal stress on anxiety- and depressive-like behaviours are sex-specific in prepubertal rats. *J Neuroendocrinol*, **30**.

116. Nazeri,M., Shabani,M., Ghotbi Ravandi,S., Aghaei,I., Nozari,M. and Mazhari,S. (2015) Psychological or physical prenatal stress differentially affects cognition behaviors. *Physiol Behav*, **142**, 155–160.